Available online at www.sciencedirect.com
SCIENCE DIRECT
Polymer 46 (2005) 10727–10732
polymer
www.elsevier.com/locate/polymer

Catalytic electroxidation pathway for the polymerization of polypyrrole in the presence of ultrafine silver nanoparticles

Hsun-Tsing Lee, Yu-Chuan Liu*

Department of Chemical and Materials Engineering, Vanung University, 1, Van Nung Road, Shuei-Wei Li, Chung-Li City, Taiwan, ROC

Received 19 July 2005; received in revised form 31 August 2005; accepted 8 September 2005
Available online 3 October 2005

Abstract

In this work, we report the first electrochemical polymerization of polypyrrole (PPy) on Au substrates in aqueous solutions containing additives of prepared Ag nanoparticles with a diameter less than 2 nm. Due to the effect of Ag nanoparticles, which can provide a catalytic electroxidation pathway for the polymerization of PPy, the synthesized PPy film demonstrates some novel characteristics. It shows a finer and granular raspberry morphology with nano-scaled particles, and a rougher surface. The conductivity of PPy is significantly increased (~8 times), which also reflects on the extremely high oxidation level of 0.35 revealed from the analysis of X-ray photoelectron spectroscopy (XPS). The mechanism of the nucleation and growth was investigated to explain the specific characteristics of PPy films.

Keywords: Polypyrrole; Ag nanoparticles; Mechanism of the nucleation and growth

1. Introduction

Among a number of conducting polymers (CPs), polypyrrole (PPy), has attracted considerable attention because it offers reasonably high conductivity and has fairly good environmental stability, and it can be widely used in batteries [1,2], supercapacitors [3,4], sensors [5,6], anhydrous electrorheological fluids [7], microwave shielding, and corrosion protection [8,9]. Moreover, it is possible for forming homopolymers or composites with optimal chemical and physical properties [10,11]. There are two methods used to synthesize PPy, chemical and electrochemical polymerizations. The principal advantage of the electrochemical method is related to the better conducting properties and long-term stability of conductivities [12,13]. However, in the electrochemical method, metals such as silver and aluminum, which oxidize more readily than the pyrrole monomer, would obviously not be good choices for the anode [14]. As we know, the electrical conductivity of PPy is attributed to the electrons hopping along and across the polymer chains with conjugating bonds [9,10]. As a result, more positively charged PPy, more electron holes available, longer polymer chains and more coplanarity between interchains, are favorable for a higher conductivity performance. The conductivity of oxidized PPy can be increased to a level of 10^3 S cm^{-1}, or higher, depending on the method of preparation and the doped ion [15–17]. Meanwhile, in order to achieve a new function of PPy, one of the most efficient means is to prepare PPy-based composite films into which new chemical components, such as nanoparticles of Fe_2O_3 and Pd [18,19] or nanostructured clays [20,21], are introduced.

In the past decade, nanostructured materials have been the focus of scientific research [22,23] due to their unusual properties of optical [24], chemical [25], photoelectrochemical [26], and electronic [27] properties. The developed methods for nanoparticles fabrication include chemical reduction [28], sonochemical reduction [29], laser ablation [30], annealing from high-temperature solutions [31], metal evaporation [32], and Ar^+ ion sputtering [27], etc. In the previous studies of the preparations of metals nanoparticles in aqueous solutions [33–35], we reported the size-controlled synthesis of Au, Ag, and Au–Ag alloy nanoparticles from their bulk substrates by sonoelectrochemical methods. It was found that fine silver nanoparticles with diameters less than 2 nm can be prepared in 0.1 M HCl aqueous solutions. To our knowledge, the effects of the additives of metal nanoparticles in electrolytes on the preparation of CPs have not yet been investigated so far. The object of this work is to electrochemically prepare PPy film on Au substrates in aqueous solutions containing prepared Ag nanoparticles. The distinguishable characteristics of

* Corresponding author. Tel.: +886 3 4515811x540; fax: +886 3 4514814.
E-mail address: liuyc@msa.vnu.edu.tw (Y.-C. Liu).

0032-3861/$ - see front matter © 2005 Elsevier Ltd. All rights reserved.
doi:10.1016/j.polymer.2005.09.031

the prepared PPy, including the nucleation and growth mechanisms, the surface morphology, and the increased conductivity, are discussed.

2. Experimental

2.1. Chemical reagents

Pyrrole (Py) was triply distilled until a colorless liquid was obtained and was then stored under nitrogen before use. HCl was used as received without further purification. The reagents (p.a. grade) were purchased from Acros Organics. All of the solutions were prepared using deionized 18.2 MΩ cm water provided from a MilliQ system.

2.2. Preparation of Ag nanoparticles

All of the electrochemical experiments were performed in a three-compartment cell at room temperature, 22 °C, and were controlled by a potentiostat (model PGSTAT30, Eco Chemie). First, a sheet of silver with bare surface area of 4 cm^2, a sheet of 2×4 cm^2 platinum, and a KCl-saturated silver-silver chloride (Ag/AgCl) rod were employed as the working, counter, and reference electrodes, respectively. Before the oxidation-reduction cycles (ORC) treatment, the silver electrode was mechanically polished (model Minimet 1000, Buehler) successively with 1 and 0.05 μm of alumina slurries to a mirror finish. Then the electrode was cycled in a deoxygenated aqueous solution of 100 mL containing 0.1 M HCl from −0.3 to +0.3 V vs Ag/AgCl at 5 mV s^{-1} for 30 scans without any duration at the cathodic and anodic vertexes. After this roughening procedure, Ag- and Cl-containing complexes were left in this aqueous solution. Immediately, without changing the electrolyte, the silver working electrode was replaced by a platinum substrate with the same bare surface area of 4 cm^2, and a cathodic overpotential of 0.2 V from the open circuit potential (OCP) of ca. 0.61 V vs Ag/AgCl was applied under sonication and a slight stirring for 20 min to synthesize Ag nanoparticles in solutions. The ultrasonic irradiation was performed by using an ultrasonic generator (model XL2000, Microson) and operated at 20 kHz with a barium titanate oscillator of 3.2 mm diameter to deliver a power of 100 W.

2.3. Electropolymerization of PPy films on Au substrates

After the preparation of Ag nanoparticles in a solution, 0.1 M pyrrole (C_4H_5N) was immediately dissolved with slightly magnetic stirring in this solution for 15 min. During this step, the solution was deoxygenated with highly pure nitrogen. Then the PPy was electrochemically polymerized at 0.85 V vs Ag/AgCl on Au substrates in this Ag nanoparticles-containing aqueous solution. For comparison, pure PPy was also polymerized on Au substrates by using the same preparation condition as mentioned above, but without the Ag nanoparticles in the polymerization electrolyte. After each step the electrode was rinsed thoroughly with deionized water, and then dried in a vacuum oven for 1 h. The samples were then placed in a sealed chamber with an oxygen free atmosphere for further measurements.

2.4. Characteristics of Ag nanoparticles and PPy films

Ultraviolet–visible absorption spectroscopic measurements were carried out on a Perkin–Elmer Lambda 25 spectrophotometer in 1 cm quartz curvettes. Before conductivity measurements, the PPy films were stripped from the electrodes with clear adhesive tapes. They had a mechanical stability that made them well suited for the measurements. The conductivities of PPy films were determined by using a four-probe technique with a direct current (Dc) measurement at room temperature. The surface morphology of PPy films was obtained using scanning electron microscopy (SEM, Model S-4700, Hitachi) and an atomic force microscope (AFM, Nanoscope III, Digital Instrument) was used to determine the surface roughness. The mean roughness was determined from the mean value of the surface relative to the center plane, which is automatically calculated from a program attached to the instrument. Raman spectra were obtained using a Renishaw inVia Raman spectrometer employing a He–Ne laser of 1 mW radiating on the sample operating at 632.8 nm and a charge-coupled device (CCD) detector with 1 cm^{-1} resolution. For the X-ray photoelectron spectroscopy (XPS) measurements a Physical Electronics PHI 1600 spectrometer with monochromatized Mg K_α radiation, 15 kV 250 W, and an energy resolution of 0.1–0.8% $\Delta E/E$ was used. To compensate for surface charging effects, all XPS spectra are referred to the C1s neutral carbon peak at 284.6 eV. The complex XPS peaks are deconvoluted into component Gaussian peaks using a peak separation and analysis software (PeakFit v4.0, AISN Software Inc.). In the XPS N 1s deconvolution, the four component peaks are located at ca. 398.2, 399.9, and at higher than 401 eV with equal value of half width at half-maximum (HWHM) to the utmost. In some situation, the peak position is prior to the equal HWHM.

3. Results and discussion

3.1. Sonoelectrochemical preparation of Ag nanoparticles

In ORC treatment, the chloride electrolyte was selected because, as for silver, this facilitates the metal dissolution-deposition process that is known to produce surface-enhanced Raman scattering (SERS)-active roughened surfaces [36]. As shown in spectrum a of Fig. 1, the absorbance maximum of Ag-containing complexes appears approximately at 291 nm, which is markedly different from that of zero-valent Ag located at ca. 410 nm [37,38] and can be confirmed from the XPS analysis. After applying a cathodic overpotential of 0.2 V, the absorbance band of Ag-containing complexes at 291 nm disappears, as shown in spectrum (b) of Fig. 1. It can be ascribed to the complete reduction of Ag-containing complexes. However, the resulting ultrafine Ag(0) nanoparticles are too small to exhibit any surface plasmon absorption

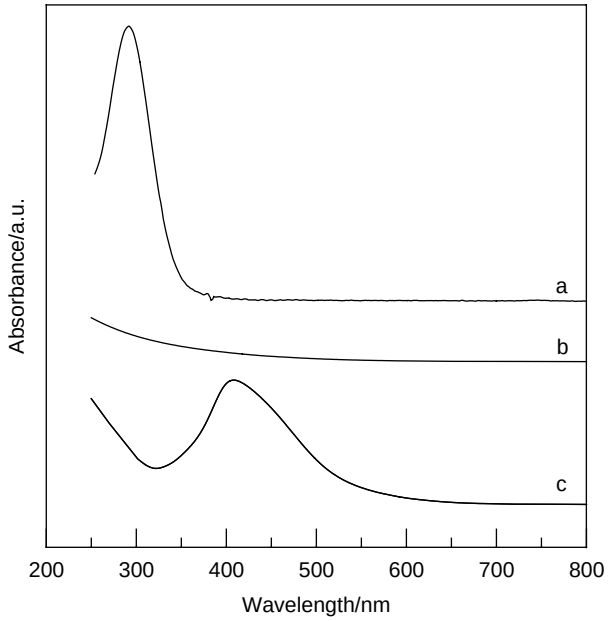

Fig. 1. UV–vis spectra of Ag-containing colloidal solutions: (a) Ag-containing complexes after roughing the Ag substrate; Ag nanoparticles synthesized by sonoelectrochemical reduction at different cathodic overpotentials of (b) 0.2 V and (c) 0.6 V from the OCP of 0.61 V vs Ag/AgCl in the solution containing Ag complexes prepared in this work.

[39]. By applying a more cathodic overpotential of 0.6 V, the appearance of the characteristic absorbance maximum at ca. 409 nm, as shown in spectrum (c) of Fig. 1, confirms that the elemental Ag(0) nanoparticles can be readily synthesized by the electrochemical reduction at room temperature under ultrasonication in the solution containing Ag complexes prepared in this study. In the case of applying a cathodic overpotential of 0.2 V, the mean particle size is less than 2 nm. Other detailed discussions were shown in the previous study [34].

3.2. Characteristics of prepared PPy films on Au substrates

Fig. 2(a) shows the typically granular raspberry morphology of pure PPy [17,40]. However, the PPy film prepared in a solution containing Ag nanoparticles exhibits a distinguishable finer granular raspberry morphology with nano-scaled particles, and a rougher surface, as indicated in Fig. 2(b). This finer structure would be responsible for a rougher surface obtained. Further AFM analyses show that the mean surface roughness of the prepared PPy film can be increased from 5.40 to 7.41 nm in adding the Ag nanoparticles in the polymerization electrolyte. The finer and rougher surfaces are of benefit in applications.

It is also known that the nucleation and growth mechanism of conducting polymers are very similar to those of metals [41,42]. Thus the mechanism for conducting polymer growth can be proved using the theory model of metal growth [43,44]. As shown in the literature [41,42], there are two kinds of nucleation, namely instantaneous and progressive, and two types of growth, such as two-dimensional (2D) and three-dimensional (3D). The number of nuclei in the instantaneous nucleation mechanism is constant, and they grow on their former positions on the bare

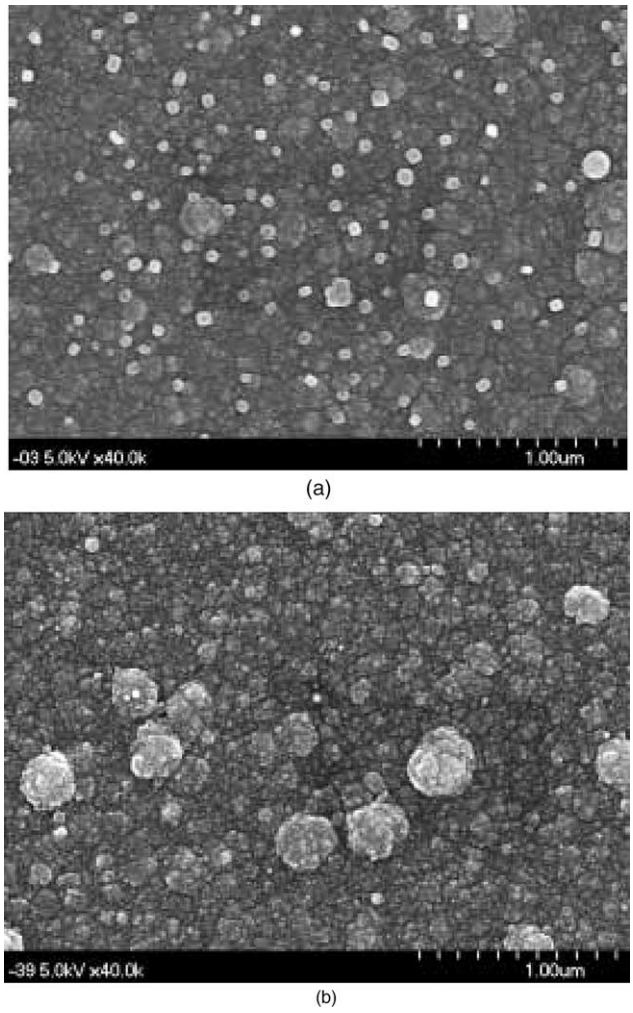

Fig. 2. SEM micrographs of electropolymerized PPy in aqueous solutions containing different electrolytes: (a) in 0.1 M HCl and 0.1 M pyrrole; (b) in 0.1 M HCl, 0.1 M pyrrole, and containing Ag nanoparticles.

substrate surface without the formation of new nuclei. Hence the radii of the nuclei are larger and the surface morphology is rougher. In progressive nucleation, the nuclei not only grow on their former positions on the bare substrate surface but also on new nuclei which form smaller nuclei particles and the surface morphology is flatter. The current maximum (i_m) for the electropolymerization of pyrrole in different electrolytes obtained from the chronoamperometric curves are compared and fitted with the theoretical curves of 2D and 3D nucleation and growth obtained from those equations derived by Harrison and Thirsk [42] for current-time relation, as shown in Fig. 3. It is clear that before the nuclei overlapping (i_m), the experimental curves for both PPy films are more or less consistent with the theoretical curve of the 3D instantaneous nucleation, as shown in curve (a). However, after the nuclei overlapping, the experimental curves for PPy films prepared in electrolytes with and without Ag nanoparticles are governed by 3D instantaneous and progressive nucleation models, as shown in curves (a) and (b), respectively. These different mechanisms may result in the flatter and the rougher surface morphologies obtained, as shown in Fig. 2(a) and (b), respectively.

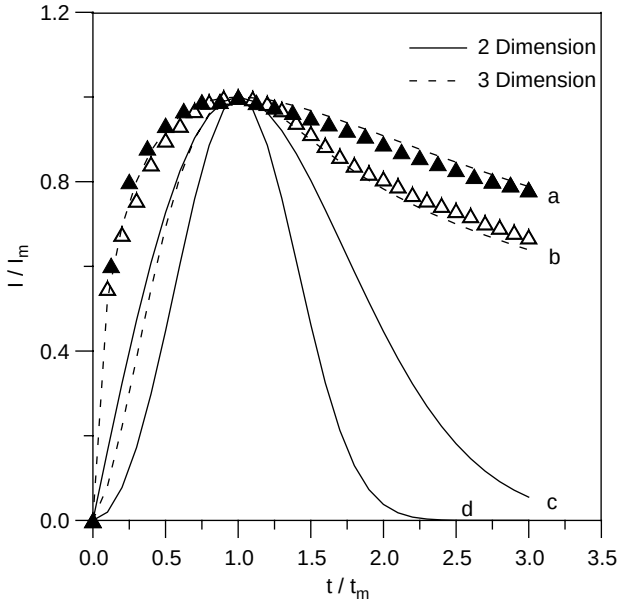

Fig. 3. Dimensionless plots of *I–t* curves for pyrrole polymerized on Au substrates in different electrolytes at 0.85 V vs Ag/AgCl, as compared with theoretical models for nucleation. Solid and hollow triangles represent the polymerizations in solutions with and without Ag nanoparticles, respectively. Curves (a) and (b) represent 3D instantaneous and progressive models (dashed lines), respectively. Curves (c) and (d) represent 2D instantaneous and progressive models (solid lines), respectively.

Meanwhile, the nucleation and growth rate of PPy in the presence of Ag nanoparticles is quite large and fast (times to i_m are 0.8 and 1.0 s for the PPy polymerizations in solutions with and without the addition of Ag nanoparticles, respectively). It may be ascribed to the catalytic effect of Ag nanoparticles, as discussed below.

Fig. 4 shows the cyclic voltammograms of pyrrole oxidized in different electrolytes. They indicate that ca. 0.6 and 0.75 V

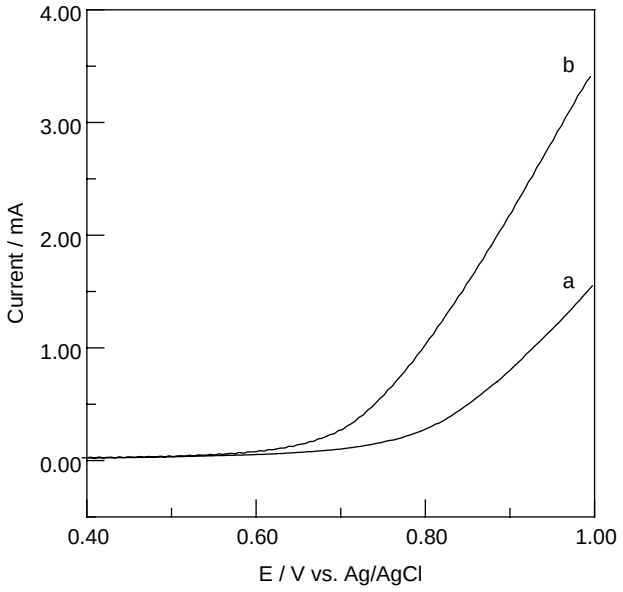

Fig. 4. *I–E* curves for pyrrole polymerized on Au substrates in different electrolytes: (a) in 0.1 M HCl and 0.1 M pyrrole; (b) in 0.1 M HCl, 0.1 M pyrrole, and containing Ag nanoparticles.

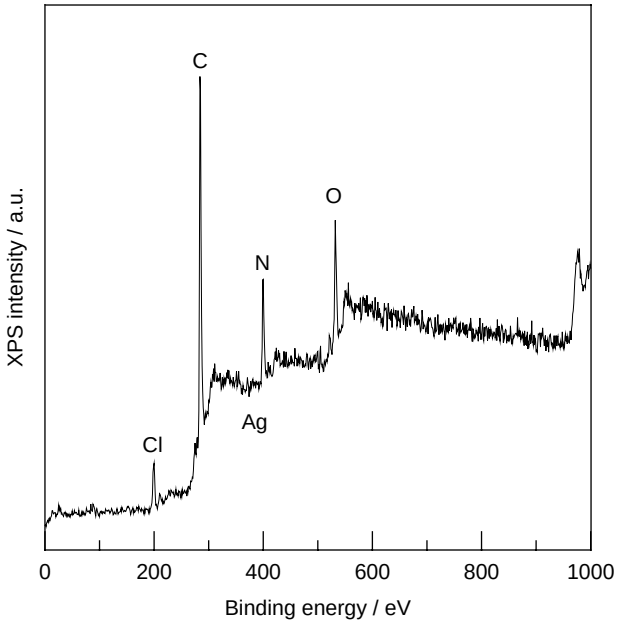

Fig. 5. XPS survey spectrum of electropolymerized PPy in aqueous solutions containing 0.1 M HCl, 0.1 M pyrrole, and Ag nanoparticles.

vs Ag/AgCl were the onset potentials of pyrrole polymerized on Au substrates in solutions with and without the addition of Ag nanoparticles, respectively. It clearly explicates that the Ag nanoparticles provide a catalytic electroxidation pathway for the PPy polymerization. Therefore, at the same applied anodic potential of 0.85 V vs Ag/AgCl in this work, the higher polymerization overpotential takes the advantage of a higher oxidation level, as discussed later, and an increased conductivity of PPy obtained. The results indicate that the conductivities of 4000 mC cm^{-2} PPy films deposited on Au substrates in solutions with and without the addition of Ag nanoparticles are 125 and 14.3 S cm^{-1}, respectively. The conductivity of PPy is significantly increased (~8 times) due to the effect of Ag nanoparticles. Meanwhile, a lower onset potential for the polymerization of PPy in Ag nanoparticles-containing solutions means a lower anodic potential is necessarily used to prepare oxidized PPy at a required conductivity. Thus, metal substrates can be widely employed for the polymerization of PPy.

Fig. 5 shows the XPS survey spectrum of PPy prepared in a solution containing Ag nanoparticles. The characteristic N, C and Cl signals of PPy are markedly demonstrated. The signal of O is generally shown in the XPS spectrum even though the sample is free of oxygen. However, the weak signal of Ag means that less Ag nanoparticles were incorporated into the PPy film during polymerization. Actually, detailed spectrum of Ag nanoparticles in the PPy composite film was also performed to confirm the presence of less Ag nanoparticles in the PPy composite film. Further analysis of the surface chemical compositions in XPS reveals that the content of Ag nanoparticles in PPy is less than 3 mol%.

Fig. 6 shows the XPS N 1s spectra of electropolymerized PPy prepared in solutions with and without the addition of Ag nanoparticles. With further deconvolution of N 1s spectra into

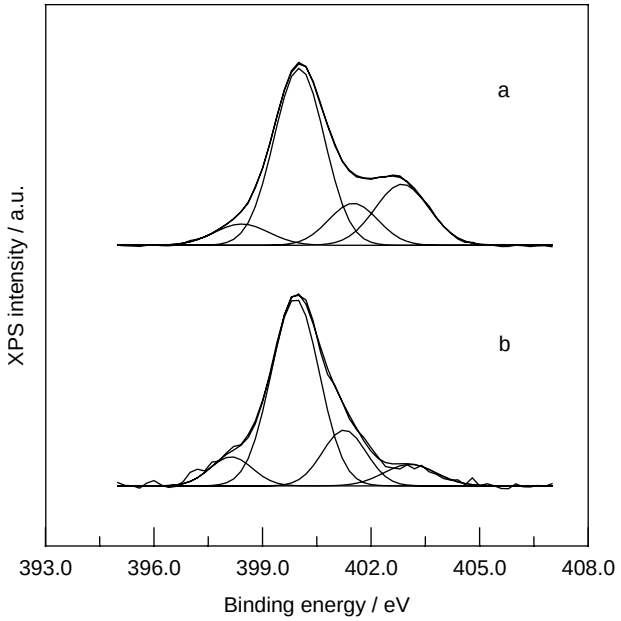

Fig. 6. XPS N 1s core-level spectra of electropolymerized PPy in aqueous solutions containing different electrolytes: (a) in 0.1 M HCl, 0.1 M pyrrole, and containing Ag nanoparticles; (b) in 0.1 M HCl and 0.1 M pyrrole.

four component peaks, the positively charged nitrogen ($-N^+H-$) species with the higher binding energy (BE) tail (BE > 401 eV) can be used to determine the oxidation level of PPy. This oxidation level is calculated from the ratio of the peak area of N^+(BE > 401 eV) to that of the total N 1s shown in the XPS spectrum [45,46]. The result shows that the oxidation level of PPy prepared in an Ag nanoparticles-containing solution is 0.35, which is significantly higher in comparison with that of 0.26 of PPy prepared in a solution without the Ag nanoparticles. The oxidation level of as-grown PPy generally ranges from 0.25 to 0.33 [47]. This higher oxidation level is reasonable for the corresponding enhanced conductivity obtained [47].

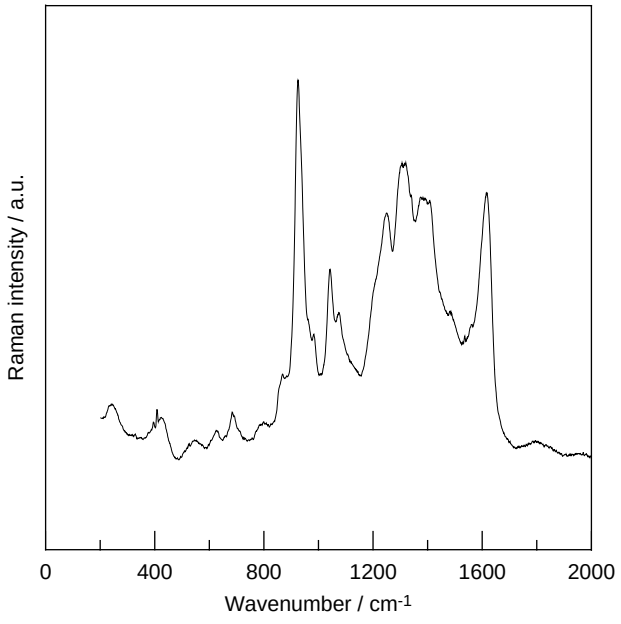

Fig. 7. Raman spectrum of electropolymerized PPy in an aqueous solution containing 0.1 M HCl, 0.1 M pyrrole, and Ag nanoparticles.

Fig. 7 shows the Raman spectrum of PPy prepared in solution containing Ag nanoparticles [48,49]. The broader Raman peaks of PPy appearing in the range of 1000–1150 cm^{-1} and 1300–1410 $cm^{-1}$are assigned to the C–H in-plane deformation and the ring stretching, respectively. The peak at about 1600 cm^{-1} is assigned to the C=C backbone stretching of PPy. No marked peaks changes are observed indicate that the Ag nanoparticles act as an electrocatalytic role in the polymerization of PPy.

4. Conclusion

First, we use a developed sonoelectrochemical pathway to synthesize Ag nanoparticles with diameter less than 2 nm in an aqueous solution from an Ag substrate. Then pyrrole monomers were added in the same solution to prepare PPy films on Au substrates. Encouragingly, the synthesized PPy films demonstrate some novel characteristics due to the catalytic effect of Ag nanoparticles. The prepared PPy shows a finer granular raspberry morphology with nano-scaled particles, and a rougher surface. The conductivity of PPy is significantly increased ($\sim$8 times), which also reflects on the extremely high oxidation level of 0.35. The mechanism of the nucleation and growth in polymerization of PPy was changed due to the presence of Ag nanoparticles in polymerization.

Acknowledgements

We thank the National Science Council of the Republic of China (NSC-92-2214-E-238-001) and Vanung University for their financial support.

References

[1] Kuwabata S, Tomiyori M. J Electrochem Soc 2002;149:A988.
[2] Kwon CW, Quintin M, Mornet S, Delville MH. J Electrochem Soc 2004; 151:A1445.
[3] An KH, Jeon KK, Heo JK, Lim SC, Bae DJ, Lee YH. J Electrochem Soc 2002;149:A1086.
[4] Ingram MD, Staesche H, Ryder KS. J Power Sources 2004;129:107.
[5] Liu YC, Hwang BJ, Hsu WC. Sens Actuators, B 2002;87:304.
[6] Ruangchuay L, Sirivat A, Schwank J. Synth Met 2004;140:15.
[7] Goodwin JW, Markham GM, Vinent B. J Phys Chem B 1997;101:1961.
[8] Truong VT, Lai PK, Moore BT, Muscat RF, Russo MS. Synth Met 2000; 110:1.
[9] He J, Tallman DE, Bierwagen GD. J Electrochem Soc 2004;151:B644.
[10] Romero AJF, Cascales JJL, Otero TF. J Phys Chem B 2005;109:907.
[11] Liu YC, Tsai CJ. Chem Mater 2003;15:320.
[12] Kuhn HH, Child AD, Kimbrell WC. Synth Met 1995;71:2339.
[13] Balci N, Bayramli E, Toppare L. J Appl Polym Sci 1997;64:667.
[14] Skotheim TA. Handbook of conducting polymers. New York: Marcel Dekker; 1986 p. 268 [chapter 8].
[15] Samuelson LA, Druy MA. Macromolecules 1986;19:824.
[16] Patil A, Ikenone Y, Wundl F, Heeger A. J Am Chem Soc 1987;109:1858.
[17] Liu YC, Huang JM, Tsai CE, Chuang TC, Wang CC. Chem Phys Lett 2004;387:155.
[18] Gangopadhyay R, De A. Eur Polym J 1999;35:1985.
[19] Cioffi N, Torsi L, Losito I, Sabbatini L, Zambonin PG, Zacheo TB. Electrochim Acta 2001;46:4205.

[20] Kim JW, Liu F, Choi HJ, Hong SH, Joo J. Polymer 2003;44:289.
[21] Trueba M, Montero AL, Rieumont J. Electrochim Acta 2004;49:4341.
[22] Guo LJ, Cheng X, Chou CF. Nano Lett 2004;4:69.
[23] Xu Q, Gates BD, Whitesides GM. J Am Chem Soc 2004;126:1332.
[24] Krolikowska A, Kudelski A, Michota A, Bukowska J. Surf Sci 2003;532–535:227.
[25] Kumar A, Mandal S, Selvakannan PR, Pasricha R, Mandale AB, Sastry M. Langmuir 2003;19:6277.
[26] Chandrasekharan N, Kamat PV. J Phys Chem B 2000;104:10851.
[27] Peto G, Molnar GL, Paszti Z, Geszti O, Beck A, Guczi L. Mater Sci Eng, C 2002;19:95.
[28] Sun Y, Mayers B, Xia Y. Nano Lett 2002;2:481.
[29] Su CH, Wu PL, Yeh CS. J Phys Chem B 2003;107:14240.
[30] Dolgaev SI, Simakin AV, Voronov VV, Shafeev GA, Verduraz FB. Appl Surf Sci 2002;186:546.
[31] Zeng H, Li J, Wang ZL, Liu JP, Sun S. Nano Lett 2004;4:187.
[32] Bourg MC, Badia A, Lennox RB. J Phys Chem B 2000;104:6562.
[33] Liu YC, Lin LH, Chiu WH. J Phys Chem B 2004;108:19237.
[34] Liu YC, Lin LH. Electrochem Commun 2004;6:1163.
[35] Liu YC, Lee HT, Peng HH. Chem Phys Lett 2004;400:436.
[36] Chang RK, Laube BL. CRC Crit Rev Solid State Mater Sci 1984;12:1.
[37] Yin B, Ma H, Wang S, Chen S. J Phys Chem B 2003;107:8898.
[38] Rivas L, Sanchez-Cortes S, Garcia-Ramos JV, Morcillo G. Langmuir 2000;16:9722.
[39] Dawson A, Kamat PV. J Phys Chem B 2001;105:960.
[40] Skotheim TA. Handbook of conducting polymer. New York: Marcel Dekker; 1986 p. 92 [chapter 3].
[41] Hwang BJ, Santhanam R, Lin YL. J Electrochem Soc 2000;147:2252.
[42] Hwang BJ, Santhanam R, Wu CR, Tsai YW. Electroanalysis 2001;13:37.
[43] Bard K, Tsakova V, Schultze JW. Electrochim Acta 1992;37:2255.
[44] Dian G, Merlet N, Barbey G, Outurquin F, Paulmier C. J Electroanal Chem 1987;238:225.
[45] Kan ET, Neoh KG, Ong YK, Tan KL, Tan BT. Macromolecules 1991;24:2822.
[46] Eaves JG, Kopelove AB. Polym Commun 1987;28:38.
[47] Skotheim TA. Handbook of conducting polymer. New York: Marcel Dekker; 1986 p. 275 [chapter 8].
[48] Liu YC, Jang LY. J Phys Chem B 2002;106:6748.
[49] Liu YC. Langmuir 2002;18:174.